Inorg. Chem. **2002**, *41*, 2087–2094

Syntheses and Characterizations of Three-Dimensional Channel-like Polymeric Lanthanide Complexes Constructed by 1,2,4,5-Benzenetetracarboxylic Acid

Rong Cao,† Daofeng Sun,† Yucang Liang,† Maochun Hong,*,† Kazuyuki Tatsumi,‡ and Qian Shi†

State Key Laboratory of Structural Chemistry, Fujian Institute of Research on the Structure of Matter, Chinese Academy of Sciences, Fujian, Fuzhou, 350002, China, and Research Center for Materials Science and Department of Chemistry, Graduate School of Science, Nagoya University, Furo-cho, Chikusa-ku, Nagoya 464-8602, Japan

Received September 27, 2001

The hydrothermal reaction of $YbCl_3 \cdot 6H_2O$ with 1,2,4,5-benzenetetracarboxylic dianhydride resulted in $[\{Yb(^{b}btec)_{1/4}(^{d}btec)_{3/6}(H_2O)_2\}_4 \cdot 6H_2O]_n$ (**1**) (H_4btec = 1,2,4,5-benzenetetracarboxylic acid), and the solvothermal reaction of $Er(NO_3)_3 \cdot 6H_2O$ or $TbCl_3 \cdot 6H_2O$ with 1,2,4,5-benzenetetracarboxylic dianhydride in H_2O/acetic acid gave rise to $[\{Er_2(^{c}btec)_{2/4}(^{e}btec)_{2/4}(^{f}btec)_{2/4}(H_2O)_4\} \cdot 4H_2O]_n$ (**2**) and $[\{Tb(H_2btec)_{2/4}(^{f}btec)_{3/6}(H_2O)\} \cdot 2H_2O]_n$ (**3**), respectively. Complex **1** crystallizes in monoclinic space group *C*2/*m* with $a = 20.8119(5)$ Å, $b = 17.6174(1)$ Å, $c = 5.7252(2)$ Å, $\beta = 92.324(1)°$, and $Z = 1$. **1** possesses a three-dimensional framework consisting of eight-coordinate ytterbium centers and two kinds of channels along the *c* axis. Complex **2** crystallizes in triclinic space group $P\bar{1}$ with $a = 9.6739(5)$ Å, $b = 11.0039(5)$ Å, $c = 11.5523$ Å, $\alpha = 104.8330(10)°$, $\beta = 91.0000(10)°$, $\gamma = 114.2570(10)°$, and $Z = 2$. **2** has a three-dimensional framework comprising both eight- and nine-coordinate erbium centers and channels along the *a* axis. Complex **3** crystallizes in monoclinic space group $P2_1/n$ with $a = 10.7246(12)$ Å, $b = 7.1693(9)$ Å, $c = 17.158(2)$ Å, $\beta = 97.109(2)°$, and $Z = 4$. **3** shows a three-dimensional framework containing nine-coordinate terbium centers and channels along the *b* axis. Uncoordinated water molecules occupy the channels in the three complexes. TGA and XRPD were determined for the three complexes, and the results illustrate that the framework of **1** is retained upon removal of uncoordinated and coordinated water molecules.

Introduction

The construction of inorganic coordination polymeric complexes has developed rapidly in recent years, owing to their interesting molecular topologies and crystal packing motifs[1] along with potential applications as functional materials.[2] As compared to the reports of d-block transition metal polymers, lanthanide polymeric complexes are less common, because the high coordination numbers of lanthanide ions may cause difficulty in controlling the synthetic reactions and thereby the structures of the products.[3] However, the fascinating coordination geometry and the interesting structures along with the special properties of lanthanide polymeric complexes have attracted increasing interest of chemists, and many studies have been reported in the literature recently.[3−7]

An assembly of metal ions and ligands in polymeric complexes can be regarded as a programmed system in which

* Author to whom all correspondence should be addressed. E-mail: hmc@ms.fjirsm.ac.cn. Fax: (+86)-591-3714946.
† Chinese Academy of Sciences.
‡ Nagoya University.

(1) (a) Hagrman, P. J.; Hagrman, D.; Zubieta, J. *Angew. Chem., Int. Ed.* **1999**, *38*, 2639. (b) Batten S. R.; Robson, R. *Angew. Chem., Int. Ed.* **1998**, *37*, 1460. (c) Yaghi, O. M.; Li, H.; Davis, C.; Richardson D., Groy, T. L. *Acc. Chem. Res.* **1998**, *31*, 474. (d) Munakata, M.; Wu, L.; Kuroda-Sowa, T. *Adv. Inorg. Chem.* **1999**, *46*, 173. (e) Blake, A. J.; Champness, N. R.; Hubberstey, P.; Li, W. S.; Withersby M. A.; Schroer, M. *Coord. Chem. Rev.* **1999**, *183*, 117.

(2) (a) Sato, O.; Iyoda, T.; Fujishima, A.; Hashimoto, K. *Science* **1996**, *271*, 49. (b) Kahn, O.; Martinez, C. *Science* **1998**, *279*, 44. (c) Evans, O. R.; Xiong, R.; Wang, Z.; Wong, G. K.; Lin, W. *Angew. Chem., Int. Ed.* **1999**, *38*, 536. (d) Fujita, M.; Kwon, Y. J.; Washizu, S.; Ogura, K. *J. Am. Chem. Soc.* **1994**, *116*, 1151.

(3) Long, D. L.; Blake, A. J.; Champness, N. R.; Schoder, M. *Chem. Commun.* **2000**, 1369.

(4) (a) Goodgame, D. M. L.; Menzer, S.; Ross, A. T.; Williams, D. J. *J. Chem. Soc., Chem. Commun.* **1994**, 2605. (b) Goodgame, D. M. L.; Menzer, S.; Smith, A. M.; Williams, D. J. *Chem. Commun.* **1997**, 339.

(5) (a) Reineke, T. M.; Eddaoudi, M.; Fehr, M.; Kelley, D.; Yaghi, O. M. *J. Am. Chem. Soc.* **1999**, *121*, 1651. (b) Reineke, T. M.; Eddaoudi, M.; O'Keefe, M.; Yaghi, O. M. *Angew. Chem., Int. Ed.* **1999**, *38*, 2590.

10.1021/ic0110124 CCC: $22.00
Published on Web 03/23/2002

the stereo and interactive information stored in the ligands is read by the metal ions through the algorithm defined by their coordination geometry.[8] Hence, the selection or design of a suitable ligand containing certain features, such as flexibility, versatile binding modes, and the ability to form hydrogen bonds,[9,10] is crucial to the construction of polymeric complexes. As known, lanthanide ions have high affinity for hard donor atoms, and ligands containing oxygen or hybrid oxygen−nitrogen atoms, especially multicarboxylate ligands,[5,11−15] are usually employed in the architectures for lanthanide polymeric complexes. 1,2,4,5-Benzenetetracarboxylic acid (H_4btec) possesses several interesting characteristics: (a) It has four carboxyl groups that may be completely or partially deprotonated, inducing rich coordination modes and allowing interesting structures with higher dimensions. (b) It can act not only as hydrogen-bond acceptor but also as hydrogen-bond donor, depending upon the number of deprotonated carboxyl groups. (c) Some of the carboxyl groups may not lie in the phenyl ring plane upon complexation to metal ions owing to space hindrance; thus it may connect metal ions in different directions. (d) It possesses high symmetry that may be helpful for the crystal growth of the product formed. Taking account of these, recently we began to assemble H_4btec and lanthanide ions into polymeric complexes under hydrothermal conditions; we hope the rich information stored in H_4btec will induce novel polymeric structures constructed by lanthanide centers. Herein we report the syntheses and characterizations of three novel three-dimensional channel-like polymeric lanthanide complexes constructed by 1,2,4,5-benzenetetracarboxylic acid, $[\{Yb(^{b}btec)_{1/4}(^{d}btec)_{3/6}(H_2O)_2\}_4\cdot 6H_2O]_n$ (**1**), $[\{Er_2(^{c}btec)_{2/4}(^{e}btec)_{2/4}(^{f}btec)_{2/4}(H_2O)_4\}\cdot 4H_2O]_n$ (**2**), and $[\{Tb(H_2btec)_{2/4}(^{f}btec)_{3/6}(H_2O)\}\cdot 2H_2O]_n$ (**3**).

Experimental Section

Materials and Analyses. All chemicals used are as purchased without purification. IR spectra were recorded on a Magna 750 FT-IR spectrophotometer as KBr pallets. Elementary analyses were carried out in the elementary analysis group of this institute.

Table 1. Crystallographic Data for Complexes **1**−**3**

complex	**1**	**2**	**3**
empirical formula	$C_{30}H_{34}O_{38}Yb_4$	$C_{15}H_{19}O_{20}Er_2$	$C_{10}H_9O_{11}Tb$
fw	1694.73	837.69	463.08
space group	*C*2/*m*	$P\bar{1}$	*P*2(1)/*n*
T (°C)	293	293	293
a (Å)	20.8119(5)	9.6739(5)	10.7246(12)
b (Å)	17.6174(1)	11.0039(5)	7.1693(9)
c (Å)	5.7252(2)	11.5523(6)	17.158(2)
α (deg)		104.8330(10)	
β (deg)	92.324(1)	91.0000(10)	97.109
γ (deg)		114.2570(10)	
V (Å^3)	2097.43(9)	1073.27(9)	1309.1(3)
Z	4	2	4
ρ_{calcd} (g cm^{-3})	1.403	2.592	2.300
λ (Å)	0.71073	0.71073	0.71073
μ (mm^{-1})	4.487	3.934	2.731
R1[a]	0.0487	0.0340	0.0498
wR2	0.135	0.0901	0.0943

[a] $R1 = \sum||F_o| - |F_c||/\sum|F_o|$, $wR2 = [\sum w(F_o^2 - F_c^2)/\sum w(F_o^2)^2]^{1/2}$, $w = 1/[\sigma^2(F_o^2) + (aP)^2 + bP]$ where $P = [\max(F_o^2,0) + 2F_c^2]/3$.

Preparation of the Complexes. $[\{Yb(^{b}btec)_{1/4}(^{d}btec)_{3/6}(H_2O)_2\}_4\cdot 6H_2O]_n$ (1). A mixture of $YbCl_3\cdot 6H_2O$ (0.048 g, 0.125 mmol), 1,2,4,5-benzenetetracarboxylic dianhydride (0.05 g, 0.25 mmol), and H_2O (16.0 mL) with a mole ratio of 1:2:7100 was heated in a stainless steel reactor with Teflon liner at 170 °C for 36 h. After cooling, colorless plate crystals of **1** were obtained. Yield: 63%. Anal. Calcd for $C_{30}H_{34}O_{38}Yb_4$: C, 21.25; H, 2.02. Found: C, 20.75; H, 2.07. IR (KBr pellet, cm^{-1}): 3649 (m), 3388 (vs), 1618 (vs), 1527 (vs), 1410 (vs), 1336 (s), 1146 (m), 850 (s), 519 (s).

$[\{Er_2(^{c}btec)_{2/4}(^{e}btec)_{2/4}(^{f}btec)_{2/4}(H_2O)_4\}\cdot 4H_2O]_n$ (2). A mixture of $Er(NO_3)_3\cdot 6H_2O$ (0.11 g, 0.25 mmol), 1,2,4,5-benzenetetracarboxylic dianhydride (0.05 g, 0.25 mmol), CH_3COOH (6.0 mL), and H_2O (10.0 mL) in a mole ratio of ca. 1:1:424:2224 was sealed in a 25 mL stainless steel reactor with Teflon liner and directly heated to 140 °C. Seven days later, the mixture was cooled to room temperature in 5 h. Pink prism-like crystals of **2** were obtained in 65% yield. Anal. Calcd for $C_{15}H_{19}O_{20}Er_2$: C, 21.51; H, 2.29. Found: C, 21.05; H, 2.34. IR (KBr, cm^{-1}): 3404 (vs), 1608 (vs), 1498 (s), 1394 (vs), 1336 (s), 1144 (m), 885 (m), 592 (s).

$[\{Tb(H_2btec)_{2/4}(^{f}btec)_{3/6}(H_2O)\}\cdot 2H_2O]_n$ (3). A mixture of $TbCl_3\cdot 6H_2O$ (0.045 g, 0.125 mmol), 1,2,4,5-benzenetetracarboxylic dianhydride (0.025 g, 0.125 mmol), CH_3COOH (6.0 mL), and H_2O (10.0 mL) in a mole ratio of ca. 1:1:848:4448 was sealed in a 25 mL stainless steel reactor with Teflon liner and directly heated to 140 °C. After 7 days, the mixture was cooled to room temperature in 5 h. Colorless prism-like crystals of **3** were obtained in 40% yield. Anal. Calcd for $C_{10}H_9O_{11}Tb$: C, 25.88; H, 1.96. Found: C, 25.37; H, 2.13. IR (KBr, cm^{-1}): 3508 (vs), 3412 (vs), 2517 (m), 1655 (vs), 1585 (vs), 1558 (s), 1398 (vs), 1126 (s), 883 (m), 839 (s), 590 (s).

Crystallographic Analyses. The intensity data of **1**−**3** were collected on a SIEMENS SMART CCD diffractometer with graphite-monochromated Mo Kα ($\lambda = 0.71073$ Å) radiation at room temperature. All absorption corrections were performed using the SADABS program.[16] The structures were solved by direct methods[17] and refined on F^2 by full-matrix least-squares using the SHELXTL-

(6) a) Liang, Y. C.; Cao, R.; Su, W. P.; Hong, M. C.; Zhang, W. J. *Angew. Chem., Int. Ed.* **2000**, *39*, 3304. (b) Decurtins, S.; Gross, M.; Schmalle, H. W.; Ferlay, S. *Inorg. Chem.* **1998**, *37*, 2443. (c) Liu, J.; Meyers, E. A.; Cowan, J. A.; Shore, S. G. *Chem. Commun.* **1998**, 2043. (d) Mao, J. G.; Song, L.; Huang, J. S. *J. Chem. Crystallogr.* **1998**, *28*, 475. (e) Liang, Y. C.; Cao, R.; Su, W. P.; Hong, M. C.; Zhang, W. J. *Chem. Lett.* **2000**, 3304. (f) Mörtl, K. P.; Sutter, J−P.; Golhen, S.; Ouahab, L.; Kahn, O. *Inorg. Chem.* **2000**, *39*, 1626.

(7) (a) Ma, B. Q.; Zhang, D. S.; Gao, S.; Jin, T. Z.; Yun, C. H. and Xu, G. X. *Angew. Chem., Int. Ed.* **2000**, *39*, 3644. (b) Pan, L.; Huang, X.; Li, J.; Wu, Y.; Zheng, N. *Angew. Chem., Int. Ed.* **2000**, *39*, 527.

(8) (a) Lehn, J. M. *Supramolecular Chemistry—Concepts and Perspectives*; VCH: Weinheim, 1995. (b) Hong, M. C.; Su, W. P.; Cao, R.; Fujita, M.; Lu, J. X. *Chem. Eur. J.* **2000**, *6*, 427.

(9) Hong, C. S.; Son, S. K.; Lee, Y. S.; Jun, M. J.; Do, Y. *Inorg. Chem.* **1999**, *38*, 5602.

(10) Moulton, B.; Zaworotko, M. J. *Chem. Rev.* **2001**, *101*, 1629 and reference therein.

(11) Kiritsis, V.; Michaelides, A.; Skoulika, S.; Golhen, S.; Ouahab, L. *Inorg. Chem.* **1998**, *37*, 3407.

(12) Benmered, B.; Guehia-Laidoudi, A.; Balegroune, F.; Birkedal, H.; Chapuis, G. *Acta Crystallogr.* **2000**, *C56*, 789.

(13) (a) Yaghi, O. M.; Li, H.; Groy, T. L. *Z. Kristallogr.—New Cryst. Struct.* **1997**, *212*, 457. (b) Duan, Z.; Wei, G.; Jin, Z.; Ni, J. *J. Less-Common Met.* **1991**, *171*, L1.

(14) Pan, L.; Woodlock, E. B.; Wang, X. *Inorg. Chem.* **2000**, *39*, 4174.

(15) (a) Daiguebonne, C.; Guilloa, O.; Gerault, Y.; Lecerf, A.; Boubekeur, K.; *Inorg. Chim. Acta* **1999**, *284*, 139. (b) Xing, Y.; Jin, Z.-S.; Duan, Z.-B.; Ni, J.-Z. *Acta Chim. Sin.* **1987**, *45*, 1044

(16) Sheldrick, G. M. *SADABS, Program for Empirical Absorption Correction of Area Detector Data*; University of Göttingen: Göttingen, 1996.

(17) Sheldrick, G. M. *SHELXS 97, Program for Crystal Structure Solution*; University of Göttingen: Göttingen, 1997.

Table 2. Selected Bonds and Angles for **1**−**3**

1[a]

Yb−O(3)#1	2.218(7)	Yb−O(7)	2.317(9)	Yb−O(8)	2.339(7)	Yb−O(1)	2.391(7)
Yb−O(4)#2	2.269(7)	Yb−O(6)	2.324(7)	Yb−O(2)	2.370(7)	Yb−O(5)	2.420(7)

O(3)#1−Yb−O(4)#2	106.9(3)	O(4)#2−Yb−O(8)	78.2(3)	O(8)−Yb−O(2)	134.0(3)	O(3)#1−Yb−O(5)	155.3(3)
O(3)#1−Yb−O(7)	85.3(3)	O(7)−Yb−O(8)	81.0(3)	O(3)#1−Yb−O(1)	79.3(3)	O(4)#2−Yb−O(5)	79.3(3)
O(4)#2−Yb−O(7)	152.4(3)	O(6)−Yb−O(8)	75.2(3)	O(4)#2−Yb−O(1)	127.6(2)	O(7)−Yb−O(5)	100.0(3)
O(3)#1−Yb−O(6)	149.3(3)	O(3)#1−Yb−O(2)	76.1(3)	O(7)−Yb−O(1)	78.3(3)	O(6)−Yb−O(5)	54.7(3)
O(4)#2−Yb−O(6)	78.4(3)	O(4)#2−Yb−O(2)	75.6(2)	O(6)−Yb−O(1)	122.1(3)	O(8)−Yb−O(5)	128.2(3)
O(7)−Yb−O(6)	78.9(3)	O(7)−Yb−O(2)	131.9(3)	O(8)−Yb−O(1)	149.1(3)	O(2)−Yb−O(5)	82.7(3)
O(3)#1−Yb−O(8)	76.4(3)	O(6)−Yb−O(2)	133.4(2)	O(2)−Yb−O(1)	55.1(2)	O(1)−Yb−O(5)	78.2(3)

2[b]

Er(2)−Er(2)#2	3.9301(6)	Er(1)−O(02)	2.395(5)	Er(2)−O(6)	2.308(5)	Er(2)−O(3)#2	2.442(5)
Er(1)−O(5)	2.223(5)	Er(1)−O(1)	2.397(5)	Er(2)−O(10)#2	2.359(5)	Er(2)−O(04)	2.462(6)
Er(1)−O(7)#1	2.229(5)	Er(1)−O(12)#2	2.452(5)	Er(2)−O(3)	2.388(5)	Er(2)−O(4)#2	2.630(5)
Er(1)−O(01)	2.295(5)	Er(1)−O(2)	2.488(4)	Er(2)−O(03)	2.391(5)		
Er(1)−O(11)#2	2.362(5)	Er(2)−O(9)	2.297(5)	Er(2)−O(2)	2.401(4)		

O(5)−Er(1)−O(7)#1	88.5(2)	O(10)#2−Er(2)−O(3)	72.74(16)	O(6)−Er(2)−O(3)#2	122.04(16)
O(5)−Er(1)−O(01)	151.4(2)	O(9)−Er(2)−O(03)	73.39(18)	O(10)#2−Er(2)−O(3)#2	73.64(16)
O(7)#1−Er(1)−O(01)	98.9(2)	O(6)−Er(2)−O(03)	80.76(19)	O(3)−Er(2)−O(3)#2	71.09(18)
O(5)−Er(1)−O(11)#2	100.85(18)	O(10)#2−Er(2)−O(03)	141.38(17)	O(03)−Er(2)−O(3)#2	144.57(17)
O(7)#1−Er(1)−O(11)#2	153.1(2)	O(3)−Er(2)−O(03)	108.67(18)	O(2)−Er(2)−O(3)#2	136.48(16)
O(01)−Er(1)−O(11)#2	85.02(19)	O(9)−Er(2)−O(2)	112.17(17)	O(9)−Er(2)−O(04)	71.01(19)
O(5)−Er(1)−O(02)	79.4(2)	O(6)−Er(2)−O(2)	80.67(17)	O(6)−Er(2)−O(04)	76.92(19)
O(7)#1−Er(1)−O(02)	77.6(2)	O(10)#2−Er(2)−O(2)	76.64(16)	O(10)#2−Er(2)−O(04)	130.88(18)
O(01)−Er(1)−O(02)	75.3(2)	O(3)−Er(2)−O(2)	70.16(16)	O(3)−Er(2)−O(04)	140.68(18)
O(11)#2−Er(1)−O(02)	128.82(19)	O(03)−Er(2)−O(2)	68.43(17)	O(03)−Er(2)−O(04)	73.20(19)
O(5)−Er(1)−O(1)	129.05(17)	O(7)#1−Er(1)−O(1)	76.7(2)	O(2)−Er(2)−O(04)	138.00(17)
O(7)#1−Er(1)−O(2)	85.11(18)	O(01)−Er(1)−O(1)	79.53(19)	O(3)#2−Er(2)−O(04)	85.39(17)
O(01)−Er(1)−O(2)	130.56(18)	O(11)#2−Er(1)−O(1)	77.83(17)	O(9)−Er(2)−O(4)#2	107.90(17)
O(11)#2−Er(1)−O(2)	72.59(16)	O(02)−Er(1)−O(1)	140.45(19)	O(6)−Er(2)−O(4)#2	71.89(16)
O(02)−Er(1)−O(2)	151.25(18)	O(5)−Er(1)−O(12)#2	76.7(2)	O(10)#2−Er(2)−O(4)#2	68.50(17)
O(1)−Er(1)−O(2)	53.28(15)	O(7)#1−Er(1)−O(12)#2	152.7(2)	O(3)−Er(2)−O(4)#2	116.50(16)
O(12)#2−Er(1)−O(2)	113.12(16)	O(01)−Er(1)−O(12)#2	84.8(2)	O(03)−Er(2)−O(4)#2	132.93(19)
O(9)−Er(2)−O(6)	143.31(18)	O(11)#2−Er(1)−O(12)#2	53.92(17)	O(2)−Er(2)−O(4)#2	139.15(16)
O(9)−Er(2)−O(10)#2	137.63(17)	O(02)−Er(1)−O(12)#2	77.24(19)	O(3)#2−Er(2)−O(4)#2	50.97(16)
O(6)−Er(2)−O(10)#2	77.77(17)	O(1)−Er(1)−O(12)#2	130.32(18)	O(04)−Er(2)−O(4)#2	63.86(18)
O(9)−Er(2)−O(3)	72.18(17)	O(5)−Er(1)−O(2)	77.36(17)		
O(6)−Er(2)−O(3)	142.30(17)	O(9)−Er(2)−O(3)#2	73.08(16)		

3[c]

Tb−Tb#2	3.9188(6)	Tb−O(11)	2.369(7)	Tb−O(1)#1	2.468(8)	Tb−O(4)#2	2.573(7)
Tb−O(10)#1	2.330(7)	Tb−O(0)	2.370(8)	Tb−O(3)#2	2.489(8)		
Tb−O(3)	2.352(7)	Tb−O(2)	2.396(7)	Tb−O(2)#1	2.550(7)		

O(10)#1−Tb−O(3)	79.5(3)	O(11)−Tb−O(1)#1	138.7(3)	O(10)#1−Tb−O(2)#1	74.8(3)
O(10)#1−Tb−O(11)	143.0(3)	O(0)−Tb−O(1)#1	82.5(3)	O(3)−Tb−O(2)#1	70.0(2)
O(3)−Tb−O(11)	90.6(3)	O(2)−Tb−O(1)#1	139.0(3)	O(11)−Tb−O(2)#1	135.0(3)
O(10)#1−Tb−O(0)	144.0(3)	O(2)−Tb−O(4)#2	110.0(2)	O(0)−Tb−O(2)#1	69.2(3)
O(3)−Tb−O(0)	89.4(3)	O(0)−Tb−O(4)#2	78.0(3)	O(2)−Tb−O(2)#1	133.63(18)
O(11)−Tb−O(0)	70.3(3)	O(1)#1−Tb−O(4)#2	67.4(2)	O(1)#1−Tb−O(2)#1	51.9(2)
O(10)#1−Tb−O(2)	71.1(3)	O(10)#1−Tb−O(3)#2	72.1(3)	O(3)#2−Tb−O(2)#1	126.2(2)
O(3)−Tb−O(2)	73.7(3)	O(3)−Tb−O(3)#2	139.65(12)	O(10)#1−Tb−O(4)#2	116.0(3)
O(11)−Tb−O(2)	71.9(3)	O(11)−Tb−O(3)#2	95.1(3)	O(3)−Tb−O(4)#2	164.5(3)
O(0)−Tb−O(2)	138.2(3)	O(0)−Tb−O(3)#2	130.1(3)	O(11)−Tb−O(4)#2	76.7(3)
O(10)#1−Tb−O(1)#1	74.2(3)	O(2)−Tb−O(3)#2	70.4(2)	O(3)#2−Tb−O(4)#2	52.0(2)
O(3)−Tb−O(1)#1	120.4(3)	O(1)#1−Tb−O(3)#2	78.8(2)	O(2)#1−Tb−O(4)#2	112.8(2)

[a−c] Symmetry transformations used to generate equivalent atoms: [a]#1 $x, y, z+1$; #2 $-x+1/2, -y+1/2, -z$; #3 $x, y, z-1$; #4 $x, -y+1, z$; #5 $-x, y, -z$; #6 $x, -y, z$. [b]#1 $x-1, y, z$; #2 $-x+1, -y+1, -z+1$; #3 $x+1, y, z$; #4 $-x, -y+1, -z+1$; #5 $-x+2, -y+2, -z+2$; #6 $-x, -y, -z+1$. [c]#1 $-x+1/2, y-1/2, -z+3/2$; #2 $-x+1/2, y+1/2, -z+3/2$; #3 $-x+1, -y-1, -z+2$; #4 $-x, -y, -z+2$.

97 program package[18] on a legend computer. All non-hydrogen atoms were refined anisotropically. The organic hydrogen atoms were generated geometrically (C−H 0.96 Å). The crystallographic data of complexes **1**−**3** are listed in Table 1, selected bonds and angles in Table 2. Crystallographic data (excluding structure factors) for the structures reported in this paper have been deposited in the Cambridge Crystallographic Data Center with CCDC Number 154398 for **1**, 169888 for **2**, and 169889 for **3**.

(18) Sheldrick, G. M. *SHELXS 97, Program for Crystal Structure Refinement*; University of Göttingen: Göttingen, 1997.

Thermal Gravimetric Analysis. Thermogravimetric analyses (TGA) were performed on a Delta Series TGA7 instrument. Powder samples were loaded into alumina pans and heated from room temperature to 650 °C at a heating rate of 10 °C/min.

X-ray Powder Diffraction Analysis. XRPD analyses were performed on D-MAX-2500 instrument at room temperature.

Results and Discussion

Syntheses. As known, the study of open framework inorganic−organic coordination polymers is one of the most

Scheme 1

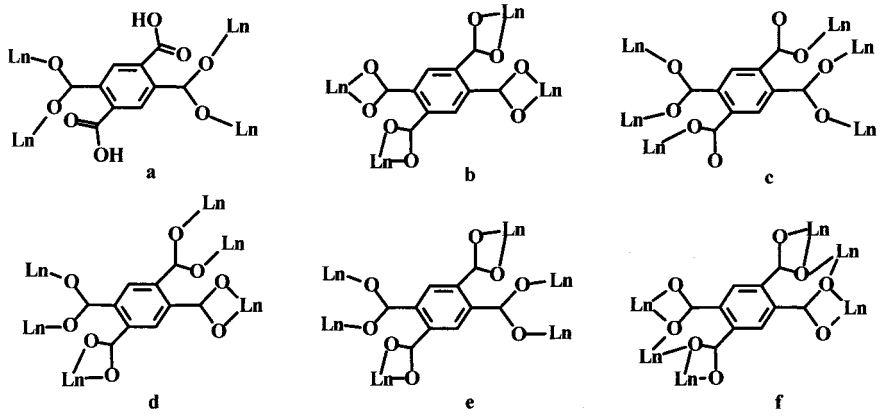

active areas in functional materials.[19] Our aim is to assemble 1,2,4,5-benzenetetracarboxylic acid and lanthanide ions into polymers with open framework structures, such as large channels capable of accommodating guest molecules. Owing to the tendency for high coordination, lanthanide ions favor the formation of condensed structures;[13,20] however, by liberating some small ligands bonded to lanthanide ions, such as water, the condensed structures can be transferred to a microporous framework.[5] Thus we focus our work on the hydrothermal reactions of group 2 (Sm−Dy) and group 3 (Ho−Lu) lanthanide series[7b] with 1,2,4,5-benzenetetracarboxylic acid. We hope that the small atomic radius and possible lower coordination number (for instance, 8 for Yb(III)) of these lanthanide ions may be helpful for the formation of less condensed structures and a microporous framework may be generated through liberating the water ligands in the products. First we determined the reaction of Yb(III). The hydrothermal reaction of $YbCl_3 \cdot 6H_2O$ and 1,2,4,5-benzenetetracarboxylic dianhydride resulted in the formation of **1** in crystalline form in good yield. As expected, two kinds of channels accommodating guest water molecules are present in **1** and the framework is retained upon removal of guest and bonded water molecules (see below). It is understandable that the $btec^{4-}$ ligand comes from the hydrolysis of its dianhydride followed by a deprotonation process in the reaction.

The successful isolation of **1** prompted us to extend our study to other group 2 and 3 lanthanide series. However, when we carried out similar reactions of $Er(NO_3)_3 \cdot 6H_2O$ and $TbCl_3 \cdot 6H_2O$ under the same reaction conditions, only uncharacterized precipitates were obtained. It has been documented that the products of hydrothermal synthesis are affected by the acidity of the reactions.[7b] Thus we tried to adjust the pH value to 4, 5, and 7 by NaOH, but no improvements of the reactions were observed. Taking account of the deprotonation process, $H_4btec \leftrightarrow H_3btec^- + H^+ \leftrightarrow H_2btec^{2-} + 2H^+ \leftrightarrow Hbtec^{3-} + 3H^+ \leftrightarrow btec^{4-} + 4H^+$, in the formation of the products, we sense that a low pH value may lower the deprotonation rate of H_4btec and thereby the formation of the products, which may be helpful for the crystal growth. Hence, the pH value was adjusted to 1 by dilute HNO_3; unfortunately almost the same result as in former reactions was observed. Although detailed studies are still needed, we propose that the unsatisfying results may arise from the quick polymerization in the reactions. In view of this, we selected acetic acid as a cosolvent, hoping it could play dual roles, one being to lower the deprotonation rate of H_4btec and the other being to form some intermediates with lanthanide ions to avoid quick polymerization. As expected, when the reactions of $Er(NO_3)_3 \cdot 6H_2O$ and $TbCl_3 \cdot 6H_2O$ were carried out in a mixed water/acetic acid solvent (pH = 2) at 140 °C for 7 days, pure well-formed crystals of **2** and **3** were obtained in satisfying yields. To confirm our speculation, we carried out the same reactions in a shorter time. When the two reactions were carried out in a period shorter than 4 days, although sometimes crystals of **2** and **3** were obtained, the yield and the purity were very bad. This result illustrates that the rates of formation of **2** and **3** are lowered in our reactions, which may be the crucial factor for the successful isolation of the two complexes in crystalline form.

Structural Description. $[\{Yb(^{b}btec)_{1/4}(^{d}btec)_{3/6}(H_2O)_2\}_4 \cdot 6H_2O]_n$ (1). Complex **1** is a three-dimensional polymer containing two types of channels with guest water molecules. All carboxyl groups of 1,2,4,5-benzenetetracarboxylic acid are deprotonated, in agreement with the IR data in which no strong absorption peaks around 1700 cm^{-1} for −COOH are observed. Two types of coordination modes of $btec^{4-}$ ligands are present in the structure: (a) each carboxylate group adopts a bidentate chelating mode, chelating one ytterbium atom ($^{b}btec^{4-}$, Scheme 1b); (b) each of two *meta*-carboxylate groups adopts a bidentate chelating mode, chelating one ytterbium atom, whereas each of the other two *meta*-carboxylate groups adopts a bidentate bridging mode, connecting two ytterbium atoms ($^{d}btec^{4-}$, Scheme 1d). An ytterbium(III) atom is coordinated by eight oxygen atoms, four from two chelating carboxylate groups of $^{b}btec^{4-}$ and $^{d}btec^{4-}$, two from bridging carboxylate groups of different

(19) (a) Seo, J. S.; Whang, D.; Lee, H.; Jun, S. I.; Oh, J.; Jeon., Y. J.; Kim, K. *Nature* **2000**, *404*, 982. (b) Noro, S.; Kitagawa, S.; Kondo, M.; Seki, K. *Angew. Chem., Int. Ed.* **2000**, *93*, 2082. (c) Li, H.; Eddaoudi, M.; O'Keeffe, M.; Yaghi, O. M. *Nature* **2000**, *402*, 276.
(20) (a) Wu, L. P.; Munakata, M.; Kuroda-Sowa, T.; Maekawa, M.; Suenaga, Y. *Inorg. Chim. Acta* **1996**, *249*, 183. (b) Seddon, J. A.; Jackson, A. R. W.; Kresinski, R. A.; Platt, W. G. *Polyhedron* **1996**, *15*, 1899. (c) Ribeiro, S. J. L.; Goncalves, R. R.; de Oliverira, L. F. C.; Santos, P. S. *J. Alloys Compd.* **1994**, *216*, 61. (d) Huskowska, E.; Glowiak, T.; Legendziewicz, J.; Oremek, G. *J. Alloys Compd*. **1992**, *179*, 13.

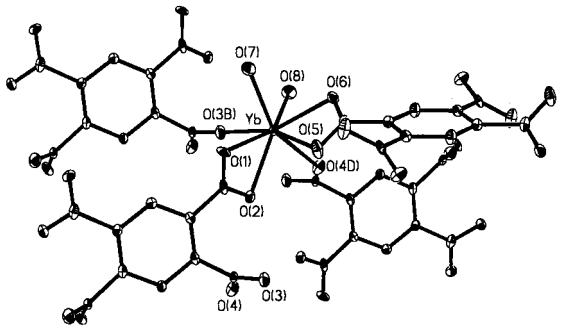

Figure 1. ORTEP plot of **1** showing local coordination environment of Yb(III) with thermal ellipsoids at 40% probability.

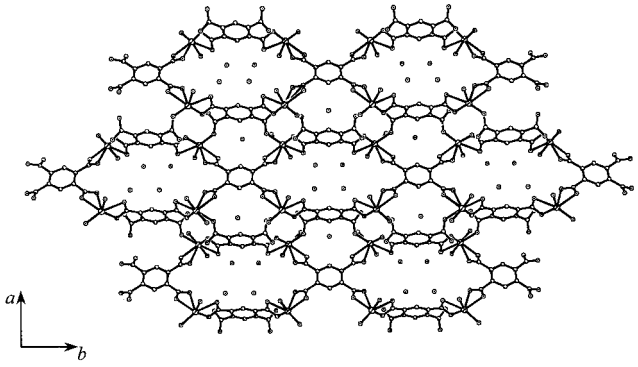

Figure 2. The 2D porous structure in **1**.

^{d}btec^{4-}, and two coordinated water molecules (Figure 1). Therefore, each ^{b}btec^{4-} acts as a μ_4-bridge linking four ytterbium centers, each ^{d}btec^{4-} acts as a μ_6-bridge linking six ytterbium centers, and each ytterbium center attaches to one ^{b}btec^{4-} and three ^{d}btec^{4-} ligands. The Yb−O bond distances range from 2.217 to 2.420 Å, similar to other related Yb−O distances.[20a] The nearest Yb···Yb distance is 4.75 Å, indicating the lack of direct metal−metal interaction. The macrocyclic unit [Yb_4(^{b}btec)$_2$(^{d}btec)$_2$(H_2O)$_8$] constitutes the basic building block of the structure. Every three Yb_4 building blocks are linked together through Yb−O bonding to induce a new small cycle, generating a two-dimensional layer structure with two kinds of pores. A large pore (cavity size of ca. 15.2 × 5.6 Å) accommodates four guest water molecules and is surrounded by six small ones, while a small pore (cavity size of ca. 8.47 × 3.4 Å) contains one guest water molecule and is shared by three large ones (Figure 2). The 2D layers are further linked together by the hoods of Yb(III) and the bridging carboxylate groups of ^{d}btec^{4-}, producing a novel three-dimensional channel-like structure along the *c* axis (Figure 3), and the channels are filled by guest water molecules. Different kinds of hydrogen bonding are observed in the structure:[21] (a) hydrogen bonding among uncoordinated water molecules in the large channels (O···O distances: 2.791(9)−2.966(9) Å); (b) hydrogen bonding of uncoordinated water molecules/coordinated water molecules (O···O distances: 2.736(8) Å for the uncoordinated water molecules in large channels and 3.006(8) Å for the uncoordinated water molecules in small channels); (c) hydrogen bonding of uncoordinated water molecules in large channels/carboxylate oxygen atoms (O···O distance: 2.741(8) Å); (d) hydrogen bonding between the two coordinated water molecules with an O···O distance of 3.023(6) Å; (e) hydrogen bonding of coordinated water molecules/carboxylate oxygen atoms (O···O distances: 2.781(6)−3.181(8) Å).

(21) Desiraju, G. R.; Steiner, T. *The Weak Hydrogen Bond*; Oxford University Press: Oxford, 2001. For hydrogen bonding, only those with O···O distances less than 3.2 Å are discussed in this paper.

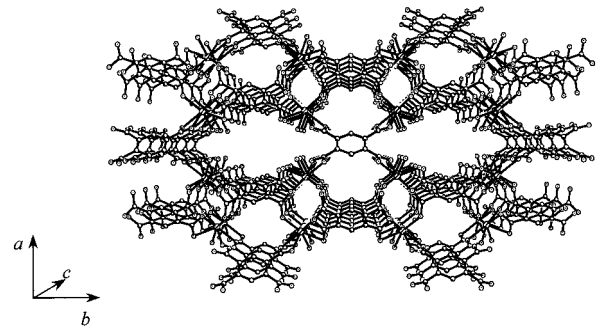

Figure 3. Packing structure along the *c* axis of **1**. Guest water molecules are omitted for clarity.

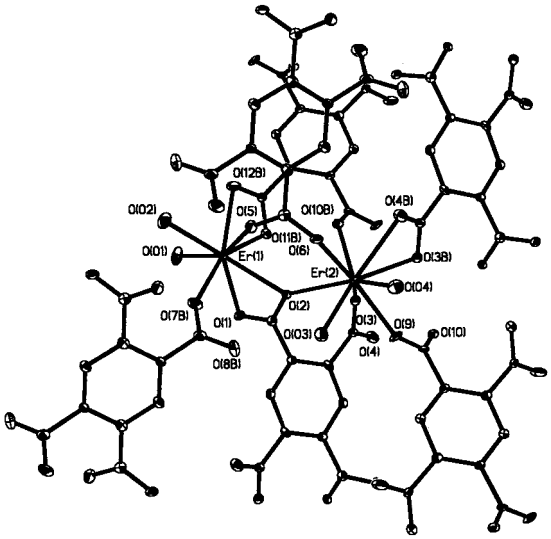

Figure 4. ORTEP plot of **2** showing local coordination environment of Er(III) with thermal ellipsoids at 40% probability.

[{Er_2(^{c}btec)$_{2/4}$(^{e}btec)$_{2/4}$(^{f}btec)$_{2/4}$(H_2O)$_4$}·4H_2O]$_n$ (2). Complex **2** is a three-dimensional polymer; the dinuclear species [Er_2(^{c}btec)$_2$(^{e}btec)$_2$(^{f}btec)$_2$(H_2O)$_4$] with interatomic distance of 3.9301(6) Å may be viewed as the building unit, as shown in Figure 4. Similar to **1**, all carboxyl groups are deprotonated and three types of coordination modes of btec^{4-} ligands are present: (a) each of two *para*-carboxylate groups adopts a monodentate mode, coordinating to one erbium atom, whereas each of the other two *para*-carboxylate groups adopts a bidentate bridging mode, linking two erbium atoms (^{c}btec^{4-}, Scheme 1c); (b) each of two *para*-carboxylate groups bridges two erbium atoms, while each of the other two *para*-carboxylate groups chelates one erbium atom (^{e}btec^{4-}, Scheme 1e); (c) each carboxylate group adopts a chelating-bridging mode, and the whole ligand connects six erbium atoms (^{f}btec^{4-}, Scheme 1f). There are two types of lanthanide environments: Er(2) is coordinated by nine oxygen atoms, one from ^{c}btec^{4-}, two from ^{e}btec^{4-}, four from ^{f}btec^{4-}, and two from coordinated water molecules. The Er(2)−O(4)#2 distance (2.630(5) Å) is quite long, while the

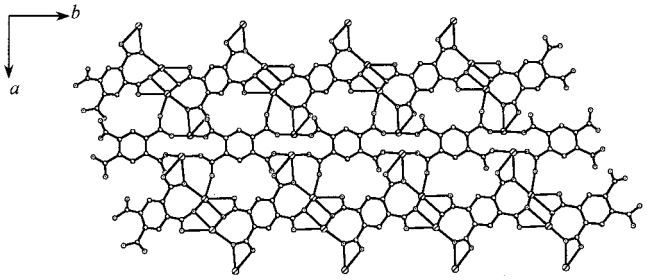

Figure 5. The 2D layer structure in **2**; water molecules are omitted for clarity

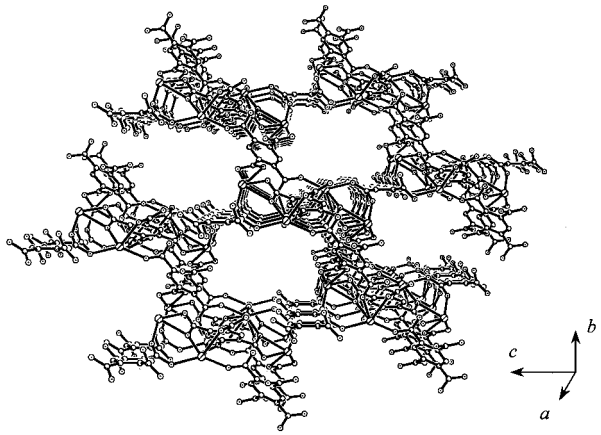

Figure 6. Packing structure along the *a* axis of **2**; water molecules are omitted for clarity.

other eight Er(2)−O distances are typical, falling in the range from 2.297(5) to 2.462(6) Å.[14,22] Er(1) is coordinated by eight oxygen atoms, two from ^{c}btec^{4-}, two from ^{e}btec^{4-}, two from ^{f}btec^{4-}, and two from coordinated water molecules, with Er(1)−O distances ranging from 2.223(5) to 2.488(4) Å. If the other two kinds of btec^{4-} ligands are neglected, each ^{f}btec^{4-} connects six Er atoms to form a [Er$_6$] subunit, every two such [Er$_6$] units are joined together through sharing two nine-coordinate Er atoms to form a linear chain, and the nine-coordinate Er atoms (Er(2)) act as linkers for the chain, whereas the eight-coordinate Er atoms (Er(1)) stand on the two sides of the chain. Every two adjacent chains are connected by ^{c}btec^{4-} through bridging eight- and nine-coordinate Er atoms by bidentate carboxylate groups and coordinating eight-coordinate Er atoms by monodentate carboxylate groups, forming a two-dimensional layer structure (Figure 5). The two-dimensional layers are further connected by ^{e}btec^{4-}, whose bridging carboxylate groups coordinate to the Er linkers of the chains and the chelating carboxylate groups coordinate to the Er atoms outside the chain, generating the final three-dimensional open framework structure with channels along the *a* axis (Figure 6). The channels possess approximate dimensions of 9.140 × 7.094 Å and are occupied by uncoordinated water molecules. There are several kinds of hydrogen bonding in **2**:[21] (a) hydrogen bonding among uncoordinated water molecules (O···O distances: 2.608(9)−2.909(9) Å); (b) hydrogen bonding of uncoordinated water molecules/coordinated water molecules (O···O distances: 2.726(8)−3.041(8) Å); (c) hydrogen bonding of uncoordinated water molecules/carboxylate oxygen atoms (O···O distances: 2.765(8)−3.132(8) Å); (d) hydrogen bonding among coordinated water molecules (O···O distances: 2.867(6)−2.894(8) Å); and (e) hydrogen bonding of coordinated water molecules/carboxylate oxygen atoms (O···O distances: 2.697(6)−2.969(6) Å for O(01), 2.694(6)−2.802(6) Å for O(02), 2.899(6)−3.025(6) Å for O(03), 2.673(6)−3.147(6) Å for O(04)). It is worth mentioning that three coordinated water molecules (O(01), O(02), and O(04)) form strong hydrogen bonds with carboxylate oxygen atoms, in agreement with TGA determination (see below).

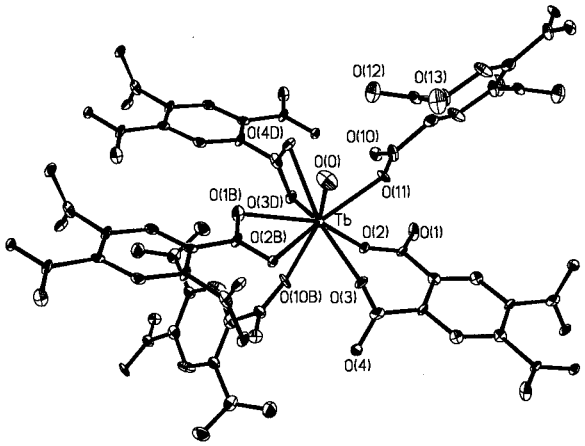

Figure 7. ORTEP plot of **3** showing local coordination environment of Tb(III) with thermal ellipsoids at 40% probability.

[{Tb(H$_2$btec)$_{2/4}$(^{f}btec)$_{3/6}$(H$_2$O)}·2H$_2$O]$_n$ (3). Complex **3** possesses a three-dimensional open framework structure consisting of nine-coordinate lanthanide centers. There are two types of coordination modes for the carboxylate ligands: (a) two *para*-carboxyl groups are not deprotonated and remain free, whereas each of the deprotonated ones bridges two terbium atoms (H$_2$btec^{2-}, Scheme 1a); (b) each carboxylate group adopts a chelating-bridging mode, and the whole ligand coordinates to six terbium atoms (^{f}btec^{4-}, Scheme 1f). The terbium atom is coordinated by nine oxygen atoms, six from ^{f}btec^{4-} ligands, two from H$_2$btec^{2-} ligands, and one from a coordinated water molecule (Figure 7). Tb−O distances range from 2.330(7) to 2.573(7) Å, similar to those in [Tb$_2$(bdc)$_3$(H$_2$O)$_4$]$_n$ and [Tb(bdc)(NO$_3$)(DMF)$_2$]$_n$ (H$_2$bdc = 1,4-benzenedicarboxylic acid).[5] There is an apparent difference between the two C−O distances of the protonated carboxyl group (C(14)−O(12) 1.236(14) Å vs C(14)−O(13) 1.318(14) Å), in agreement with the broad and strong absorption at 1655 cm^{-1} in IR for the presence of −COOH; the red shift from 1700 cm^{-1} of H$_4$btec may be caused by strong hydrogen bonding[21] between one uncoordinated water molecule and the protonated carboxyl group (O(12)···O(w1) 2.654(8) Å), which is also supported by TGA data (see below). Therefore, each ^{f}btec^{4-} ligand acts as a μ_6-bridge linking six terbium centers and each terbium center attaches to three ^{f}btec^{4-} ligands to form a two-dimensional layer structure with the nearest metal−metal distance of 3.9188(6)

(22) (a) Hawthorne, F. C.; Borys, I.; Ferguson, R. B. *Acta Crystallogr. C* **1983**, *39*, 540. (b) Sugita, Y.; Ouchi, A. *Bull. Chem. Soc. Jpn.* **1987**, *60*, 171.

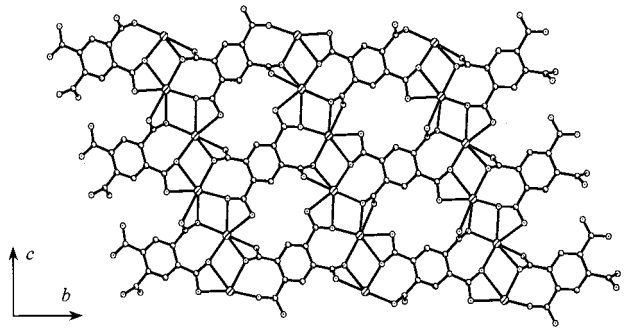

Figure 8. The 2D layer structure in **3**; water molecules are omitted for clarity.

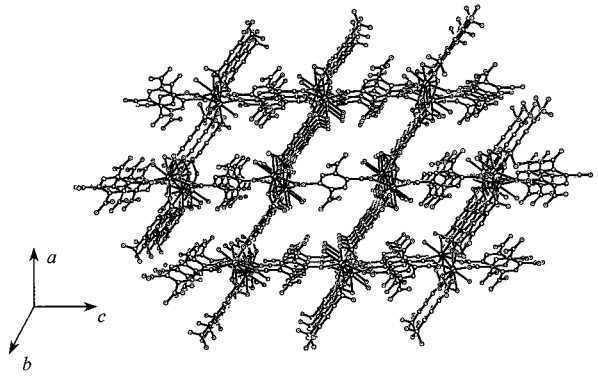

Figure 9. Packing structure along the *b* axis of **3**; guest water molecules are omitted for clarity.

Å. The layer can also be viewed as consisting of ladders sharing side pieces, in which the side pieces are formed by Tb chains and rungs by ^{f}btec^{4-} ligands (Figure 8). The two-dimensional layers are further linked by H_2btec^{2-} ligands that act as 1,4-benzenedicarboxylate, resulting in the formation of a three-dimensional open framework structure with channels along the *b* axis, and the channels are occupied by guest water molecules (Figure 9). The approximate dimensions of the channels are 12.050 × 11.196 Å. Similar to **1** and **2**, several kinds of hydrogen bonding are present in **3**:[21] (a) hydrogen bonding between the two uncoordinated water molecules with an O···O distance of 2.837(9) Å); (b) hydrogen bonding of one uncoordinated water molecule and the coordinated water molecules with an O(0)···O(w2) distance of 2.756(8) Å; (c) hydrogen bonding of uncoordinated water molecules/carboxylate oxygen atoms (O···O distances range from 2.654(6) to 3.074(8) Å); (d) hydrogen bonding of coordinated water molecules/carboxylate oxygen atoms (O···O distances range from 2.729(6) to 3.192(6) Å).

Thermogravimetric Analyses (TGA) and XRPD Results. Thermogravimetric analyses for the three complexes have been determined. For **1**, the first weight loss of 4.20% from 60 °C to 130 °C corresponds to the loss of four guest water molecules ($4H_2O/[\{Yb(^{b}btec)_{1/4}(^{d}btec)_{3/6}(H_2O)_2\}_4\cdot 6H_2O]$, calculated: 4.25%); the second weight loss of 2.04% from 160 °C to 190 °C corresponds to the loss of the other two guest water molecules ($2H_2O/[\{Yb(^{b}btec)_{1/4}(^{d}btec)_{3/6}(H_2O)_2\}_4\cdot 6H_2O]$, calculated: 2.12%); and the third weight loss of 8.36% from 220 °C to 280 °C corresponds to the loss of the coordinated water molecules ($8H_2O/[\{Yb(^{b}btec)_{1/4}(^{d}btec)_{3/6}(H_2O)_2\}_4\cdot 6H_2O]$, calculated: 8.50%). The final

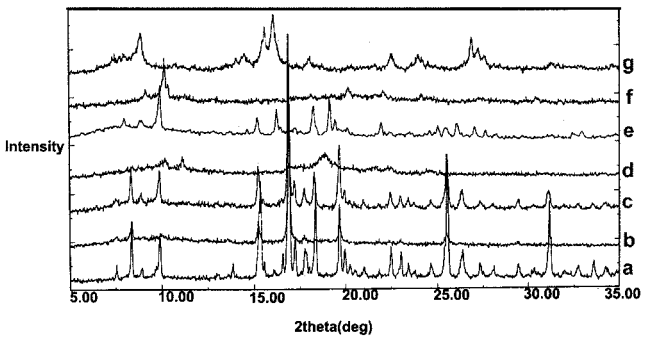

Figure 10. XPRD patterns for **1**: (a) taken at room temperature, (b) after heating 1 at 130 °C for 30 min, (c) after rehydration of sample b for 11 h, (d) after heating 1 at 200 °C for 30 min, (e) after rehydation of sample d for 48 h, (f) after heating 1 at 280 °C for 30 min, (g) after rehydation of sample f for 48 h.

weight (85.66%) leaves a framework of $[\{Yb(^{b}btec)_{1/4}(^{d}btec)_{3/6}\}_4]$ (calcd, 85.12%), which does not lose weight upon further heating to 430 °C. For **2**, the first weight loss of 2.40% from 75 °C to 104 °C corresponds to the loss of an uncoordinated water molecule ($H_2O/[\{Er_2(^{c}btec)_{2/4}(^{e}btec)_{2/4}(^{f}btec)_{2/4}(H_2O)_4\}\cdot 4H_2O]$, calcd: 2.11%); the weight loss of 8.38% from 105 °C to 141 °C corresponds to the loss of the other three uncoordinated water and one coordinated water molecules ($4H_2O/[\{Er_2(^{c}btec)_{2/4}(^{e}btec)_{2/4}(^{f}btec)_{2/4}(H_2O)_4\}\cdot 4H_2O]$, calcd: 8.44%); and the weight loss of 1.93% from 209 °C to 286 °C corresponds to the loss of one coordinated water molecule ($H_2O/[\{Er_2(^{c}btec)_{2/4}(^{e}btec)_{2/4}(^{f}btec)_{2/4}(H_2O)_4\}\cdot 4H_2O]$, calcd: 2.11%). The final weight (87.02%) leaves a framework of $[\{Er_2(^{c}btec)_{2/4}(^{e}btec)_{2/4}(^{f}btec)_{2/4}(H_2O)_2\}]$ (calcd: 87.34%). The loss of the other two coordinated water molecules in **2** is not observed before 430 °C where the decomposition starts. For **3**, the first weight loss of 3.98% from 82 °C to 128 °C corresponds to the loss of one uncoordinated water molecule ($H_2O/[\{Tb(H_2btec)_{2/4}(^{f}btec)_{3/6}(H_2O)\}\cdot 2H_2O]$, calcd: 3.88%); the second weight loss of 3.60% from 205 °C to 266 °C corresponds to the loss of the other uncoordinated water molecule ($H_2O/[\{Tb(H_2btec)_{2/4}(^{f}btec)_{3/6}(H_2O)\}\cdot 2H_2O]$, calcd: 3.88%), which is understandable: the strong hydrogen bonding between one uncoordinated water and a −COOH group of H_2btec^{2-} (O(13)···O(w1), 2.654(8) Å) may hold the water molecule more tightly. The loss of a coordinated water molecule (obsd 3.52%, calcd 3.88%) begins at 364 °C and ends at 431 °C where the decomposition of **3** starts.

Heating−cooling and dehydrate−hydrate experiments were carried out according to the TGA results and monitored by X-ray powder diffraction techniques (XRPD). As shown in Figure 10, when **1** was heated to 130 °C, four guest water molecules evolved from the sample and some characteristic XRPD peaks disappeared; however, after the sample was rehydrated, the XRPD pattern was almost the same as the original one, illustrating the complete recovery of the structure. When **1** was heated at 200 °C, all uncoordinated water molecules evolved from the sample, the XRPD pattern was broadened, and some of the characteristic peaks disappeared, but most of the important peaks were recovered after rehydration. Interestingly, although all the guest and coordinated water molecules evolved from the sample after

heating at 280 °C, some important characteristic XRPD peaks were still recovered after rehydration. Most of XRPD peaks for the second and third dehydrate−hydrate cycles possess positions similar to those of original ones; the slight shift and broadening of some peaks may be attributed to incomplete recovery of the symmetry of the structure.[5a] This phenomenon is commonly observed in zeolites, which indicates distortion of pores but does not preclude porosity and maintenance of the framework of the complex.[5a,23] The result illustrates that the main framework of **1**, [{Yb(^{b}btec)$_{1/4}$(^{d}btec)$_{3/6}$}$_4$] that does not lose weight upon heating to 430 °C as shown by TGA data is retained upon removal of guest and bonded water molecules, similar to that reported in $[Tb_2(bdc)_3(H_2O)_4]_n$.[5a]

When **2** was heated to 150 °C, all uncoordinated water molecules evolved from the sample and some characteristic XRPD peaks disappeared; however, after rehydration, the XRPD pattern was almost the same as the original one, illustrating the complete recovery of the structure. When **3** was heated at 280 °C, all uncoordinated water molecules were lost, the XRPD pattern was broadened, and some of the characteristic peaks disappeared, but almost all of the important peaks were recovered after rehydration. Heating **2** and **3** over 430 °C induces the complete decomposition of the two complexes, and XRPD cannot be recovered. These results show that the frameworks of **2** and **3** are retained on the removal of guest water molecules.

In the polymer $[Tb_2(bdc)_3(H_2O)_4]_n$ with an eight-coordinate lanthanide center, the loss of the coordinated water molecules happens at 115 °C and no alteration of the crystal structure topology of the resulting solid is observed.[5a] However, the TGA behavior of polymer with nine-coordinate lanthanide centers is quite different, in which the loss of the second coordinated water molecule on the lanthanide center is much more difficult and spans a wide temperature range.[14] Similar results are observed in our complexes. The lanthanide center in **1** is eight-coordinate, the loss of coordinated water molecules takes place before 280 °C, and the framework of the complex is retained after the loss of coordinated water molecules; whereas both **2** and **3** contain nine-coordinate lanthanide centers, and the loss of coordinated water molecules is quite difficult. The different TGA behaviors of **1**−**3** may be ascribed to the different lanthanide centers, which may cause the different strength of hydrogen bonding for coordinated water molecules. As discussed above, hydrogen bonding of coordinated water molecules/carboxylate oxygen atoms is present in the three complexes, and the strength order is **1** < **3** < **2**, e.g., carboxylate ligands in **3** and **2** hold the coordinated water molecules more tightly and cause their loss to be more difficult. One coordinated water molecule in **2** (O(03)) that has weaker hydrogen bonding with carboxylate oxygen atoms loses more easily than the other three; this may somehow support our speculation, although detailed elucidation on the difference of the TGA results still remains unclear.

(23) Breck, D. W. *Zeolite Molecular Sieves, Structure, Chemistry, and Use*; John Wiley & Sons: New York, 1974.

Conclusions

We have successfully assembled 1,2,4,5-tetracarboxylic acid and Ln(III) (Ln = Yb, Er, and Tb) into three novel three-dimensional channel-like polymeric complexes, [{Yb(^{b}btec)$_{1/4}$(^{d}btec)$_{3/6}$(H_2O)$_2$}$_4$·6H_2O]$_n$ (**1**), [{Er$_2$(^{c}btec)$_{2/4}$(^{e}btec)$_{2/4}$(^{f}btec)$_{2/4}$(H_2O)$_4$}·4H_2O]$_n$ (**2**), and [{Tb(H_2btec)$_{2/4}$(^{f}btec)$_{3/6}$(H_2O)}·2H_2O]$_n$ (**3**), where the channels accommodate guest water molecules. The reaction intermediates play a crucial role in the formation of the complexes, especially for **2** and **3**; careful selection of a second solvent in the solvothermal reaction, such as acetic acid, which may adjust the pH value of the reactions and form intermediates with lanthanide ions, is helpful for the isolation of the products in crystalline form. The different lanthanide centers in the complexes influence their TGA behaviors. The loss of coordinated water on the eight-coordinated lanthanide center in **1** is easier than the loss of coordinated water molecules on the nine-coordinate lanthanide centers in **2** and **3**. TGA and XRPD results illustrate that the framework of **1** is retained on removal of guest and bonded water molecules, indicating that the complex may be used to generate porous material.

Acknowledgment. The authors wish to thankfully acknowledge the financial support from NNSFC, the key project from CAS, Open Laboratory of Chirotechnology of the Hong Kong Polytechnic University and JSPS.

Supporting Information Available: Three X-ray crystallographic files in CIF format. This material is available free of charge via the Internet at http://pubs.acs.org.

IC0110124